MATERIALS
CHEMISTRY
FRONTIERS

RESEARCH ARTICLE

Check for updates

Tuning aggregation-induced emission nanoparticle properties under thin film formation†

Javad Tavakoli,[ab] Scott Pye, [iD][b] A. H. M. Mosinul Reza,[bc] Ni Xie,[d] Jian Qin,[c] Colin L. Raston, [iD][b] Ben Zhong Tang [iD][d] and Youhong Tang [iD] *[ab]

The most frequently used approach to preparing aggregation-induced emission fluorogen (AIEgen) particles is precipitation. Therefore, the addition of an AIEgen solution into water results in the formation of AIEgen particles in a very short time. Within such a short period of time and in the absence of proper mixing under shear, AIE particles are likely to be distributed in a wide range of sizes, thereby affecting their ultimate brightness and applications. Despite numerous attempts, the size of AIEgen particles is still within the range of 200–300 nm. For the first time, we developed a facile robust and cost-effective method for the fabrication of aggregation-induced emission nanoparticles with tuneable particle sizes <100 nm, high quantum yield, and excellent photostability. The direct diffusion of nanoparticles within the cell or in a single-celled organism, as an advantage of size reduction, opens new opportunities for biological and material studies. Such a significant reduction in AIE nanoparticle size has the potential for developing more efficient techniques for characterizing advanced nanomaterials and understanding biological processes and detection strategies.

Introduction

Fluorescence (FL) microscopy techniques have become a powerful tool for biological research and for understanding the relationship between structure and properties of materials. Nevertheless, effective employment of these techniques is limited to material and biological studies which are performed at low concentration. Therefore, a wide range of studies which aim to measure a material property or visualize a process in an aggregated state is unlikely to take advantage of those techniques. The major drawback is the irrepressible quenching of traditional FL agents in the aggregated state.[1] In a recent initiative to tackle this problem, fluorogens with aggregation-induced emission (AIE) property have been developed.[2] In contrast to the common aggregation-caused quenching (ACQ) effect, the unusual AIE effect works constructively, in that the FL of AIEgens is boosted by restriction of intramolecular rotation (RIR).[2] Highly emissive in the aggregated state, AIE fluorogens (AIEgens) develop novel

sensing strategies that function in a photoluminescence turn-on mode.[3] Over the past 10 years, researchers have successfully synthesized different AIEgens for different purposes, including lighting up an assembly process, visualizing reaction progress, measuring a material property, identifying a phase composition or detecting damage.[4–10]

The most frequently used approach to preparing AIE particles is precipitation. AIEgens are mainly soluble in an organic solvent and are insoluble in water.[11] Therefore, the addition of an AIEgen solution into water results in the formation of AIEgen particles in a very short time. Within such a short period of time and in the absence of proper mixing under shear, AIE particles are likely to be distributed in a wide range of sizes, thereby affecting their ultimate brightness and applications.[12–14] It is believed that control of AIEgen particle size during formation influences their ultimate brightness, where packing of molecules minimizes intramolecular rotation. Despite numerous attempts, the size of AIEgen particles is still within the range of 200–300 nm. One study utilized ultrasonic waves as a source of mechanical stress to form AIE crystals which were brighter than those prepared by a precipitation technique, with their size around 120 nm or greater.[15] As far as we can ascertain, there is no strategy for fabricating AIE particles <100 nm in size and the impact of particle size on FL properties of AIEgens is unclear. Thus, a major challenge is to develop a facile robust and cost-effective method for the fabrication of AIEgens with tuneable particle sizes <100 nm. Such a significant reduction in AIE nanoparticle size has the potential for developing more efficient techniques

[a] *Medical Device Research Institute, College of Science and Engineering, Flinders University, South Australia 5042, Australia.*
E-mail: youhong.tang@flinders.edu.au; Tel: +61-8-82012138
[b] *Institute for Nanoscale Science and Technology, College of Science and Engineering, Flinders University, South Australia 5042, Australia*
[c] *College of Science and Engineering, Flinders University, South Australia 5042, Australia*
[d] *Department of Chemistry, The Hong Kong University of Science and Technology, Hong Kong, China*
† Electronic supplementary information (ESI) available. See DOI: 10.1039/c9qm00585d

for characterizing advanced nanomaterials and understanding biological processes and detection strategies.

The recently developed vortex fluidic device (VFD) is a relatively inexpensive research tool for controlling chemical reactivity and selectivity, materials synthesis and probing the structure of self-organized systems, offering a range of benefits over conventional processing.[16] The dynamic thin film within the VFD microfluidic platform is generated in a rapidly rotating surface, imparting high shear stress and micro-mixing. Typically, a quartz of glass tube closed at one end is rapidly rotated at 45° tilt angle, with a finite amount of liquid in the tube, as the confined mode of the VFD, or where liquids are constantly fed into the tube, exiting at the top, as the continuous flow mode of operation. We have successfully employed the VFD for a number of diverse applications, including the fabrication of various nanocarbon materials,[17,18] intensified aqueous two-phase separation for protein purification,[19] manipulation of polymer networks,[20] exfoliation of graphite and boron nitride[21] and protein folding.[22] Of particular interest, we found that the VFD is effective for controlling the size and shape of nano-particles, for both top-down and bottom-up processing. We hypothesized that the VFD is capable of tuning and controlling the size of AIEgen particles while providing real-time insights into the effect of particle size on their FL properties. The AIEgen of choice was the ubiquitous and commercially available tetra-phenylethylene (TPE), with a view of exploring the potential for developing a new research tool for use in basic science and applications in health and environment technologies.

Results and discussion

FL signature of TPE changes under thin film formation

TPE is fully miscible in tetrahydrofuran (THF) and partially miscible in water–THF mixtures. The conventional method for preparing TPE particles involves adding water (anti-solvent) to vigorously shaken THF–TPE solution (batch processing) with the ensuing brightness of the TPE particles depending strongly on the final ratio of water to THF. Consistent with other studies using this method, an increase in the volumetric fraction of water (WF) caused TPE aggregation and changed the FL property (Fig. 1(a)), with the FL intensity negligible for WF < 80% then increasing in tracking towards WF 98% (emission wavelength $\lambda_{em} = 470$ nm and excitation wavelength $\lambda_{ex} = 350$ nm). Tuning the fraction of anti-solvent to solvent (water–THF) is the most effective method to control the fluorescence of TPE for which the unique FL signature is fixed under batch processing. Contrary to this understanding, we find that under intense micro-mixing and high shear in the VFD that the FL signature of TPE does not depend merely on the water–THF ratio (Fig. 1(b)). Briefly, water was added to a rapidly rotating 20 mm diameter glass tube (17.5 mm ID) tilted at 45° relative to the horizontal position as the optimal angle for all VFD processing[23] at a predetermined speed and desired film thickness. TPE nanoparticles were pre-pared by adding dropwise a THF–TPE solution to the preformed thin water f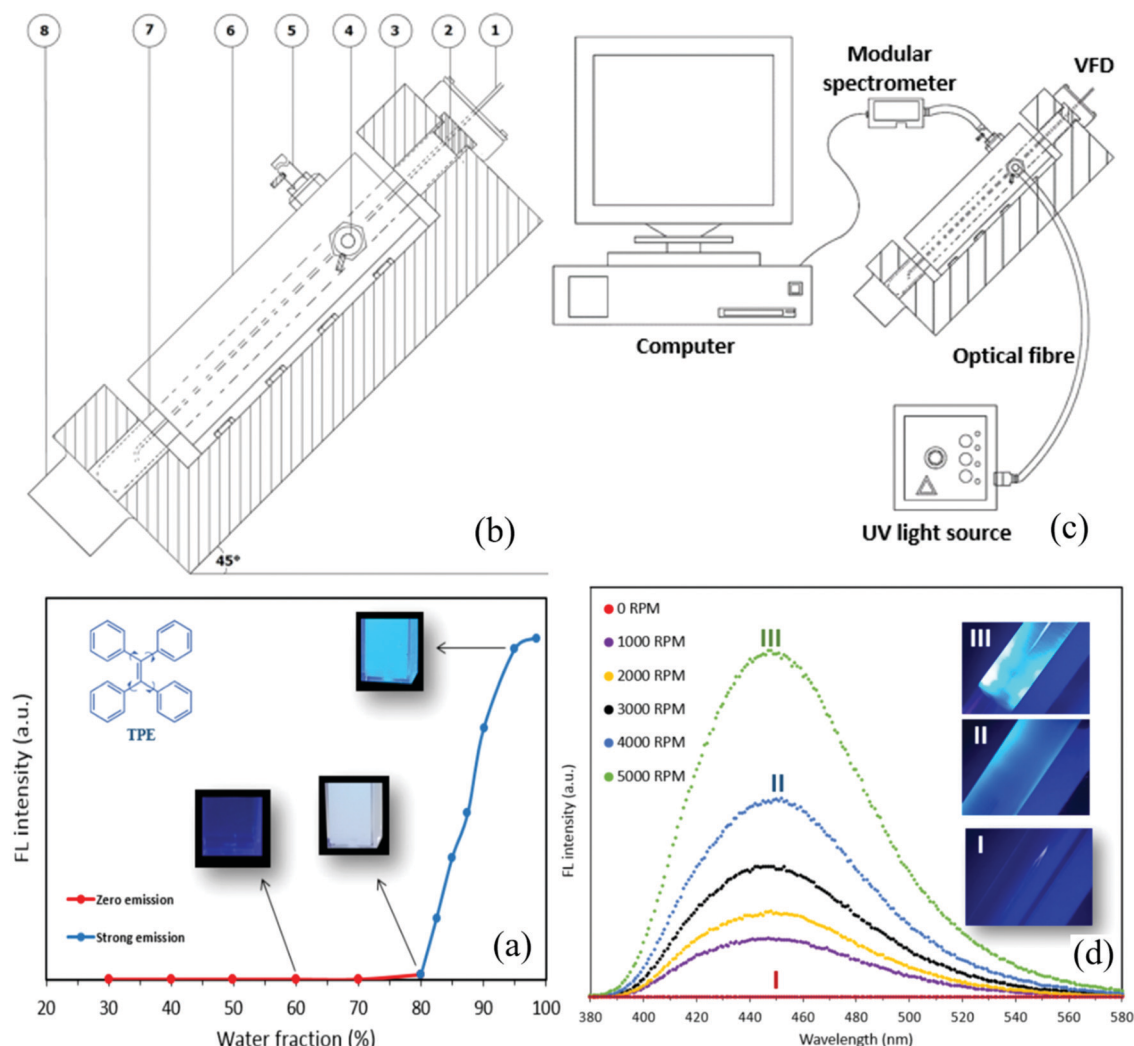ilm in the VFD. The FL property of the particles was measured *in situ* using optical fibres and a modular spectrometer (Fig. 1(c)) with special attention paid to minimizing THF, and water, evaporation during the formation of TPE particles (Supplementary S1, ESI†).

To demonstrate the utility of using the VFD method for preparing TPE nanoparticles with FL property, we explored the specific ratio of THF to WF at 60%, noting this ratio does not result in any FL using the conventional batch processing (Fig. 1(a)). Surprisingly, strong FL was observed using the VFD-mediated processing, dramatically increasing rotational speed from 1000 to 5000 rpm (Fig. 1(d), Supplementary Movie M1, ESI†). Enhanced emission from the TPE particles was observed, revealed by an increase in FL maxima.

Tuning nanoparticle size of TPE in VFD

Further investigations revealed that the changes in the FL of TPE particles were not limited to the 60% THF–water fraction, with similar findings at different THF–water fractions and different variable rotation speeds (Fig. 2(a)). When the THF–water fraction is <40%, there was no emission, as for TPE particles prepared by both traditional batch processing. In the present study, for water fractions >50% there is a direct relationship between rotation speed and the FL intensity of the TPE particles. We established that increasing the rotational speed significantly increased the FL maxima of the solutions (Supplementary S2, ESI†). For a THF–water fraction of 50%, with the tube rotating at 5000 rpm during the formation of TPE particles resulted in approximately 9 times greater FL maxima compared to that of TPE particles which were prepared at 0 rpm rotation and same THF–water fraction (Fig. 2(b)), with no-emission for solutions prepared using batch processing. When the THF–water fraction was 95%, there was a 114% enhancement of the FL maxima of TPE particles prepared at 5000 rpm relative to solutions prepared under batch processing (0 rpm) (Fig. 2(c)). We found that for all selected water fractions (50–95%), the trend in FL intensity was increasing. However, for high water fractions >90%, the increasing rate in FL intensity was lower compared to that of low water fractions (Supplementary S2, ESI†). We also evaluated the effect of varying water fraction on the FL maxima (ultimate brightness) of solutions of TPE particles at different rotational speeds (Fig. 2(d)), establishing that for all rotational speeds, an increase in water fraction resulted in higher maximum relative intensity. For traditionally prepared TPE particles, when the rotation speed was 0 rpm, a 40-times increase in the FL maxima was observed at WF = 95% compared to that of TPE particles which were prepared at WF = 80%. For water fractions <80% the associated emissions were zero, with a weak emission at 80% water fraction. Surprisingly, we found that VFD-derived solutions of TPE particles were FL active for THF-water fractions <80% (up to WF = 40%). At constant rotation speeds above 1000 rpm, an increase in water fraction resulted in an increase of both FL maxima (Supplementary S3, ESI†) and maximum relative intensity. The highest maximum relative intensity for VFD-derived TPE particles was *ca.* 190 times greater for THF–water fraction and rotation speed at 90% and 5000 rpm, respectively.

We found that the size of TPE particles prepared using the traditional batch method were in the range 359 ± 43 to 190 ±

538 | *Mater. Chem. Front.,* 2020, **4**, 537–545

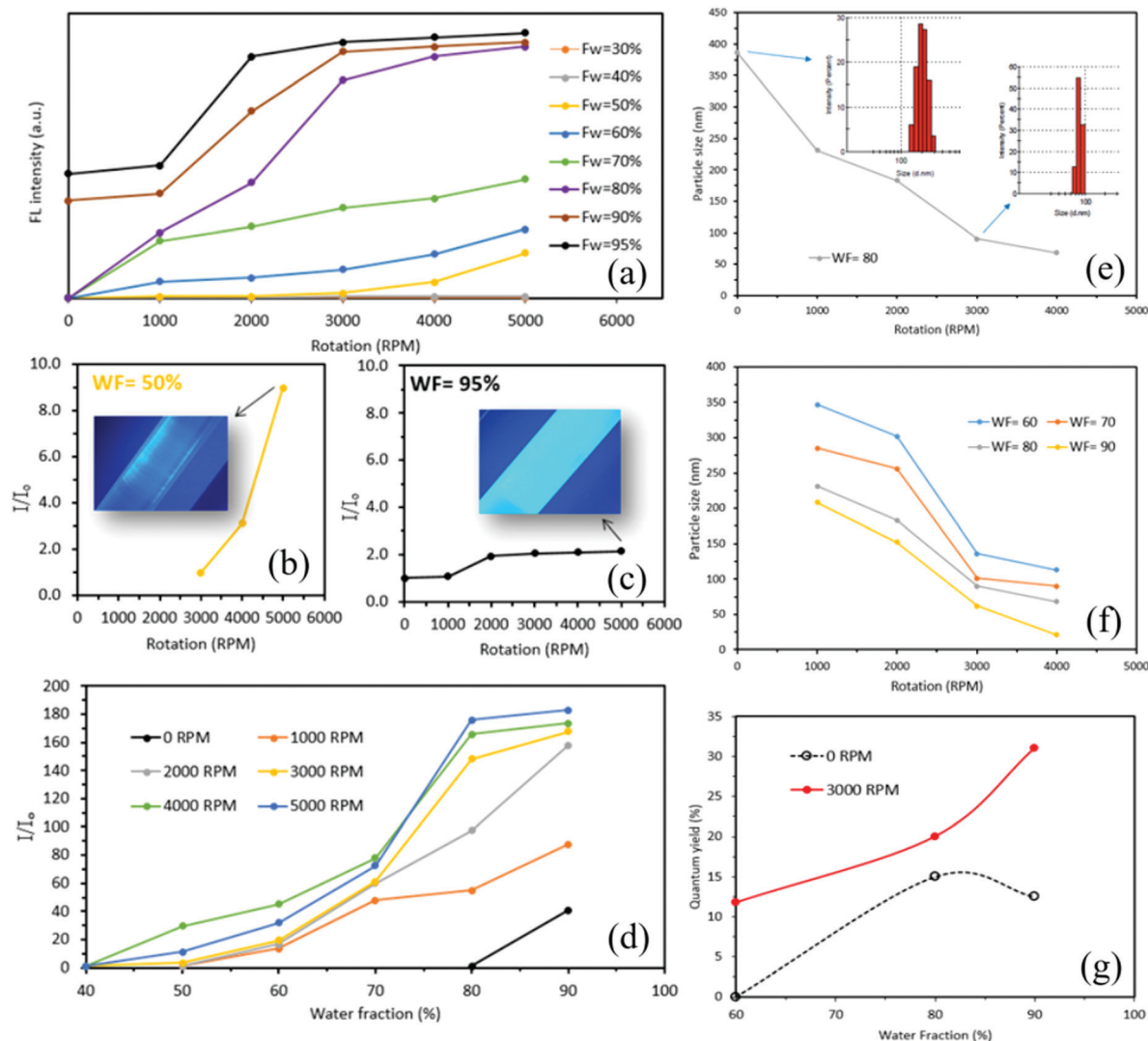This journal is © The Royal Society of Chemistry and the Chinese Chemical Society 2020

Fig. 1 (a) The FL signature of TPE prepared under batch processing for different water fractions in THF. Strong emission occurs for WF > 80%, with weak emission for 70% < WF < 80%, and negligible <70%. The FL photograph insets were taken under UV illumination, λ 365 nm, highlighting the brightness of solutions relative to WF. (b) Schematic of a vortex fluidic device (VFD) combined with a spectrophotometer for *in situ* measurement of FL of TPE particles highlighting 1, a jet feed inlet, 2, a tube cap, 3, a tube holder, 4 a spectroscope optic fibre inlet for excitation, 5, a spectroscope optic fibre outlet for collecting emitted spectrum, 6, an optic fibre holder and isolator, 7, a VFD tube (20 mm diameter), and 8, an electrical motor. (c) Schematic of the VFD and modular spectrometer assembly in (b) and (d) FL spectra for different rotation speeds in the VFD for a THF/water fraction of 60%, revealing a direct relationship between rotation speed and FL properties, along with images captured by a camera under UV light, Ex 365 nm.

39 nm (Supplementary S4, ESI†). The VFD-mediated method herein resulted in a significant decrease in TPE particle size with increasing rotational speed of the tube, for the water fraction at 80% (Fig. 2(e)). The size of the TPE particles at 0 rpm was 384 nm, slightly larger than those prepared using the above rigorously stirred method. At 1000 rpm, the size of the particles formed was significantly less at ca 260 nm, reducing further for increasing rotational speeds, with 3000 and 4000 rpm affording *ca.* 93 and 68 nm, respectively. The captured images using a FL microscope at different rotation speeds were consistent with what we observed for the reduction of TPE particle size (Supplementary S5, ESI†). We also performed different experiments to evaluate the effect of water fraction and rotation speed on the size of the TPE particles (Supplementary S6–S10, ESI†). For a constant water fraction, increasing the rotation speed resulted

in a reduction of particle size (Fig. 2(f)). A WF of 60% gave 352 nm at 1000 rpm and 113 nm at 4000 rpm, with corresponding values for 70% and 90% water fraction, 285 and 90 nm, and 210 and 21 nm, respectively. Of particular note is a ten-times reduction in size for 90% water fraction in going from 1000 to 4000 rpm, and that for a particular rotational speed, the size of the TPE particles reduces when the water fraction is increased (Supplementary S11, ESI†). Subsequently, we found that the fluorescence quantum yield of TPE nanoparticles was significantly boosted by the VFD-mediated method (Fig. 2(g) and Supplementary S12, ESI†).

While the fluorescence quantum yield of TPE nanoparticles, prepared by the conventional batch method in THF–water fraction = 60%, was almost negligible,[24] it was boosted to 11% when the VFD-mediated method with the rotation speed

This journal is © The Royal Society of Chemistry and the Chinese Chemical Society 2020

Mater. Chem. Front., 2020, **4**, 537–545 | **539**

Fig. 2 Effect of rotation speed and water fraction on the FL of solutions of TPE particles (a) change in the FL maxima at different rotation speeds and constant water fractions. Change in the relative FL maxima as a function of rotation speed at (b) 50% and (c) 95% water fraction. (d) Change in relative intensity of FL as a function of water fraction at constant rotation speeds. Effect of the rotation speed of the VFD tube on the size of the TPE particles. (e) Reduction of the particles size by increasing rotational speed for the water fraction at 80%. (f) The relationship between TPE particle size and rotation speed at different water fractions. (Inset: Distribution of TPE particles prepared at 0 and 3000 rpm rotation speeds.) (g) The fluorescence quantum yield (%) measured for VFD-mediated (red line) and the conventional batch (dot line) methods at different water fractions.

of 3000 rpm was employed. Noted that the increase of the fluorescence quantum yield was almost 2.6 times higher for VFD-mediated TPE nanoparticles@3000 rpm compared to that of those prepared by the conventional batch method at THF–water fraction of 90%. A summary of the properties of the TPE nanoparticles was presented in Table 1. Our further investigation, using a polarising microscope, revealed that TPE nanoparticles that are formed by the VFD-mediated method were in the crystalline state. The small blue shift that was found in the FL spectra indicating an increase in the crystallinity of TPE nanoparticles (Supplementary S13, ESI†). It is likely that the observation of higher FL maxima for VFD-mediated TPE nanoparticles was relevant to the formation of smaller crystals with narrow size distribution that resulted in relatively tight packing of TPE molecules. We also found acceptable stability

for the TPE nanoparticles, with less than 5% decrease in the FL maxima over 20 days (Supplementary S14, ESI†), which is critical to cell imaging and biomedical applications. A negligible reduction in FL maxima was found after 5 h for TPE nanoparticles were fabricated at WF = 80% and 3000 rpm rotational speed. Less than 5% drop in FL maxima was seen for these nanoparticles after 480 h indicating relatively high FL stability over time.

Cell imaging and tracking

One of the main challenges of traditionally prepared AIEgens is their large size, which makes their penetration into cells problematic thereby limiting their biomedical applications despite their biocompatibility. Herein we used *Euglena gracilis* for the pilot cell studies, a species of single-celled alga that has been widely used for such purposes in the literature.[25] The aim

Table 1 Summary of the properties of TPE nanoparticles prepared using VFD compared to those of prepared by the traditional method

| Water fraction (%)	FL intensity (a. u.)	Average particle size (nm)	Relative intensity I/I_0	Selected QY (%)
4000 rpm				
90	534	21	173.4	42.43
80	510	68	165.6	—
70	210	90	78.1	—
60	93	113	45.3	11.75
3000 rpm				
90	517	62	167.7	—
80	459	93	148	19.84
70	190	105	61.3	—
60	60	140	19.45	—
2000 rpm				
90	395	150	158	
80	244	180	97.6	13.84
70	150	260	60.1	—
60	42	300	19.1	—
1000 rpm				
90	220	210	87.6	—
80	138	260	54.9	3.88
70	120	285	47.8	—
60	34	352	13.54	—
0 rpm				
90	205	190	41	15.29
80	5	384	1	0.97
70	0	—	0	0
60	0	—	0	0

was to evaluate whether VFD-derived TPE particles <100 nm in size can penetrate inside *Euglena*, noting that *Euglena* has a flexible pellicle containing microtubules that allow it to absorb food directly through the cell surface *via* phagocytosis. The physical characteristics of *Euglena* were identified by SEM prior to the FL studies, with their average size 30 ± 5 μm and microtubules <100 nm in size, average 85 ± 12 nm (Fig. 3(a1)–(a4)).

It is well understood that 4 different types of the chlorophyll–protein complex are available within the structure of *Euglena*.[26] These complexes have FL properties and their associated emission maximum was seen at 682–718 nm upon excitation at the wavelength of 400–500 nm. Since TPE emits light at 450 nm when excited at 350 nm, the FL property of different *Euglena* samples was carefully examined for the excitation wavelengths of 350 and 450 nm. Images of different samples were captured by FL microscope at 0 (light only), 350 and 450 nm excitations (Fig. 3(b)). Light microscopy imaging of control samples in the absence of TPE particles revealed the presence of *Euglena* (Fig. 3(b1)). Upon excitation at 350 nm, the captured image was entirely black with no evidence of TPE particles, as expected (Fig. 3(b2)). *Euglena* had no FL under the 350 nm wavelength excitation; however, when excited at the wavelength of 450 nm, the green light was emitted (Fig. 3(b3)). When *Euglena* was placed in a solution containing TPE nanoparticles 69 ± 8 nm in size for 2 h (water fraction = 90%, and subjected to 3000 rpm), penetration of TPE nanoparticles into *Euglena* was found (Fig. 3(b4) and (b5)). Separate images (at 0 and 350 nm excitations) were captured in order to distinguish the FL of TPE nanoparticles

within the *Euglena*. Blue dots in the *Euglena* represented TPE nanoparticles that had penetrated inside the *Euglena*. No penetration inside *Euglena* was found for traditionally prepared TPE particles larger than 300 nm (water fraction = 80% and rotation speed = 0 rpm) after 4 h (Fig. 3(b6) and (b7)). Further investigation revealed that the penetration of TPE nanoparticles and their accumulation within *Euglena* increased after 4 h compared to after 1 h (Fig. 3(c1) and (c2)). The TPE nanoparticles were 69 ± 8 nm in size and prepared at 3000 rpm (water fraction = 90%). In addition, TPE nanoparticles <30 ± 12 nm (ω = 4000 rpm, WF = 95%) penetrated into *Euglena* more efficiently than the larger 90 ± 25 nm nanoparticles (ω = 2000 rpm, WF = 80%) after 2 h (Fig. 3(c3) and (c4)).

VFD-mediated fabrication of AIE nanoparticles

To further understand the impact of different rotational speeds in the VFD on the formation of TPE nanoparticles, a high-speed camera was employed and associated images with application of an edge detection Laplacian filter were captured at different time points (Fig. 4(a)). Technically, the filter is a 2-D isotropic measure of the second spatial derivative of an image that highlights regions of rapid intensity change and is therefore often used for edge detection. As observed from the captured images, a drop of TPE–THF solution turned into numerous smaller drops after hitting the thin layer of water in the VFD (Supplementary Movie M2, ESI†). When the rotation speed was high (4000 rpm), the drop size was significantly smaller, and the drops were more isolated than with lower rotation speed (2000 rpm). Indeed, at lower rotation speeds, the TPE–THF solution fitted into the flow stream of water, resulting in the creation of small regions that were likely continuous (Fig. 4(a) and Supplementary Movie M3, ESI†). This was obvious after post-processing (particle analysis) of the images using open-source ImageJ software (Fig. 4(b)-insert). The forces applied to the TPE–THF drop due to the rotation of water are likely to be the main cause of this phenomenon (Supplementary S15, ESI†). On the basis of the simplified theoretical modelling for estimation of the resultant forces applied to the TPE–THF drop by rotating water (Supplementary S15, ESI†), the resultant forces dramatically increased with an increase in rotation speed. The estimated resultant force at 4000 rpm (420 N) was approximately 28 times greater than that estimated at 1000 rpm (15 N). The results obtained from image analysis were consistent with the model, revealing that an increase in the magnitude of the resultant forces exerted on a TPE–THF drop led to the formation of more isolated and smaller regions rich in THF in the surrounding water. When both the rotation speed and water fraction were high (4000 rpm and 90%, respectively), THF-rich regions were small and surrounded by a large amount of antisolvent (water). This is consistent with TPE molecules being aggregated and encapsulated in a smaller volume. With an efficient micro-mixing process under shear, the size of these small volumes was likely to decrease, resulting in the formation of TPE aggregates at nanoscale and recovery of the FL property. In contrast, with low rotation speed (2000 rpm), THF-rich regions formed approximately continuous regions that were connected to each other with isolated regions larger than the regions
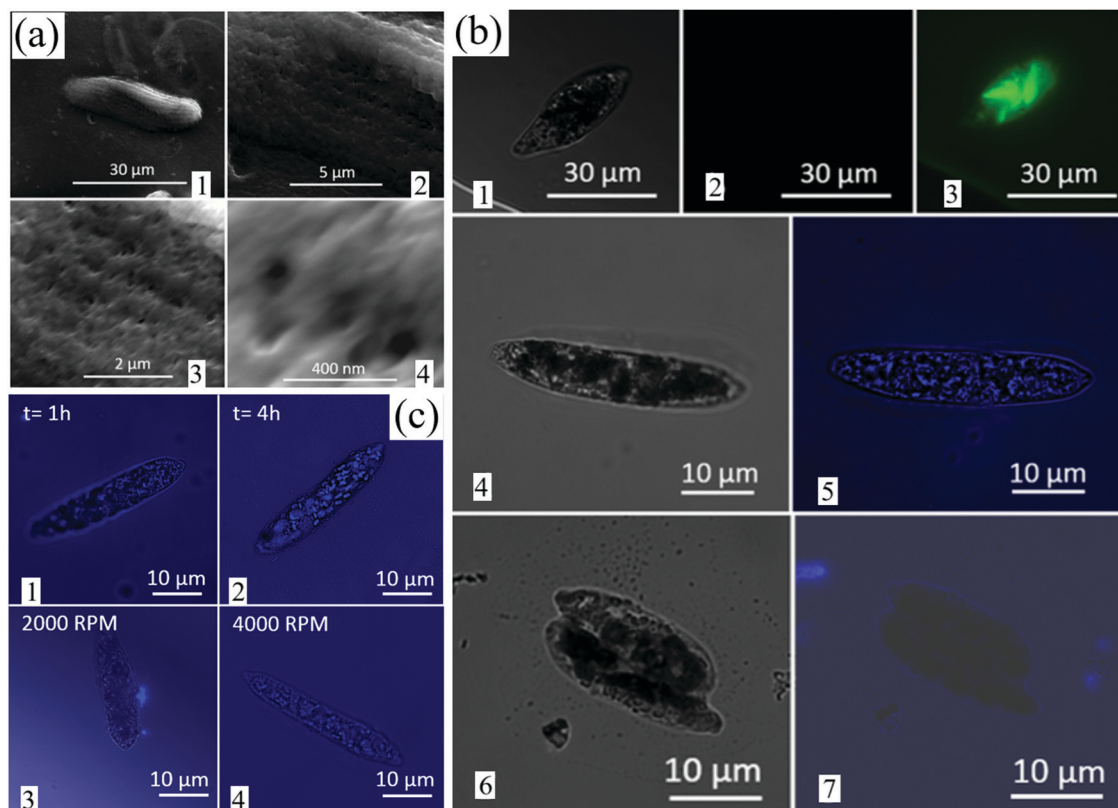
Fig. 3 (a) SEM images of *Euglena gracilis* captured under different magnifications. Micro-tubular structure of pellicle is seen at (3) 2 μm and (4) 400 nm scale bars revealing an average particle size diameter of 85 ± 12 nm. (b) Light and FL microscope images of *Euglena gracilis*. (1) Light and FL microscopic images under (2) 365 nm and (3) 470 nm excitation wavelengths captured from the control sample (without TPE particles). (4) and (5) Represent captured light and FL (λ_{exc} = 365 nm) microscopic images of a *Euglena gracilis* soaked in TPE–THF–water mixture prepared under 3000 rpm rotation at water fraction = 90% (size of TPE particles = 69 ± 8 nm) for 2 h. (6) and (7) show light and FL (excited at 365 nm) microscopic images of *Euglena gracilis* that were treated with TPE particles use traditional batch processing (0 rpm, water fraction = 80% and particle size > 300 nm) for 2 h and (c) effect of soaking time and particle size on the penetration of TPE particles into *Euglena*. (1) and (2) FL images of *Euglena gracilis* placed in a solution of VFD-driven TPE nanoparticles (3000 rpm, water fraction = 90% and particle size = 69 ± 8 nm) at different time points of 1 and 4 h, respectively. After 2 h soaking of *Euglena gracilis* into two different sizes of TPE nanoparticles (3) particle size = 90 ± 25 nm (ω = 2000 rpm, WF = 80%) and (4) particle size = 30 ± 12 nm (ω = 4000 rpm, WF = 95%), more penetration is seen for the smaller particle size.

developed at higher rotation speeds. The aggregation of TPE molecules more likely occurs only at the THF–water interface. Molecules on the surface of nanoparticles (200–400 nm in size) are likely to emit light upon excitation and contribute to the FL of the aggregates (Fig. 4(c)), and this would explain why increasing the water fraction (decreasing the THF) together with a rising rotation speed resulted in higher emission and stronger FL properties. We have established a facile penetration of very small aggregates of TPE into the structure of single-celled algae, but not so for the larger TPE particles. This has the potential for the brighter tracking of cells, as well as their distribution in different parts of the cell. (Supplementary S16, ESI†).

Experimental

Materials and reagents

1,1,2,2-Tetraphenylethylene (TPE, CAS no. 632.51.9) and tetrahydrofuran (THF) were purchased from Sigma-Aldrich, Australia. *Euglena gracilis* were a generous gift from the Biological Sciences Laboratory, Flinders University, Australia.

Preparation of TPE stock solution

A stock solution of TPE in THF at 100 mM was prepared by dissolving 1.662 g of TPE in 50 mL THF. The solution was stored in a refrigerator at 4 °C for further use.

Preparation of TPE particles by the traditional method

Aliquots of the stock solution were transferred to 5 mL volumetric flasks. After appropriate amounts of THF were added, the final aliquot solutions were added to water dropwise and under stirring to furnish 20 μM solutions with different water fractions (10–95%). FL of traditionally prepared TPE particles was detected at different water fractions using an FL spectrophotometer (Cary Eclipse, Agilent Technologies) at the excitation wavelength of 350 nm (λ_{ex}). The emission wavelength was 450 nm (λ_{em}).

VFD-mediated preparation of solutions of TPE particles

A VFD was used to prepare a thin film of water. The VFD housed an angled rotating borosilicate glass tube (20 and 17.5 mm outer and inner diameter, respectively, 19.4 cm in length,
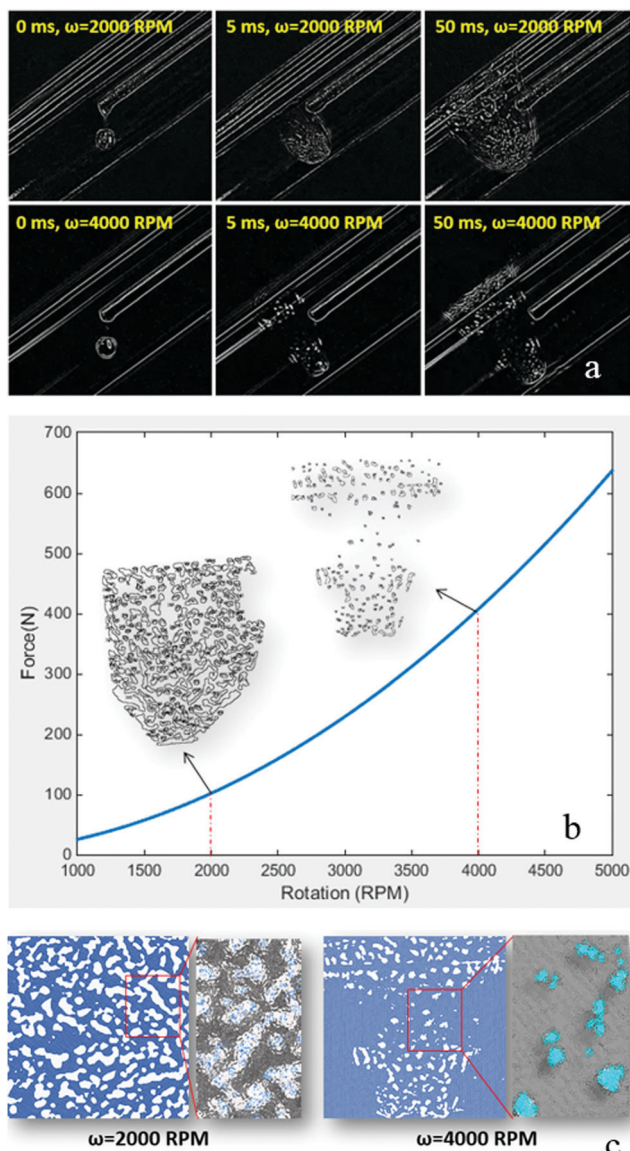
Fig. 4 Modelling and schematic illustration of the formation of TPE nanoparticles at different rotational speeds. (a) Images captured by a high-speed camera at 2000 and 4000 rpm. (b) Modelling of resultant forces exerted on a TPE–THF drop after landing in rotating water in the VFD (insets: post-processed images indicating regions rich in TPE–THF that were formed after injection). (c) Schematic illustration of the formation of particles within regions rich in THF and encapsulated in water.

inclined at 45° relative to the horizontal position). By precisely varying the rotational speed of the tube and adjusting the solution to anti-solvent volume fraction, TPE particles were readily generated. Briefly, 2 mL of water was placed in the VFD tube, the cap was inserted in place and the rotation speed was set. The TPE–THF solution was prepared as already explained (preparation of TPE particles by traditional method). After 1 min of rotation, the final aliquot solutions were added to the VFD tube (rotating water) to furnish 20 µM solutions with different water fractions (10–95%). The rotation continued for 30 s and was held constant among all samples. The FL property of the TPE particles was measured *in situ* during preparation

(30 s of rotation) using a modular USB spectrophotometer (Ocean Optics, USA), fiber optics and OceanView software. This allowed for real-time acquisition and analysis.

TPE particle size measurement

The size of the TPE particles was measured using a dynamic light scattering method, in a Malvern Zetasizer. All samples were diluted before measurement by adding one drop of a solution containing TPE particles to 2 mL of water/THF mixture. The associated water fraction was consistent with that of the undiluted samples.

High-speed camera imaging

A high-speed camera (V1212, DANTEC Dynamics) with 35 mm lens was used to capture transient phenomena at 12 600 fps within the VFD tube upon injection of the TPE–THF solution.

Culture of *Euglena gracilis*. The culture medium was prepared by mixing 30 g wheat grains, 25 g rice grains and 5 g skim milk powder into 1 L Milli Q water. Consecutively, the medium was autoclaved at 121 °C for 5 min and was stored at 4 °C for future use. Subsequently, *Euglena gracilis* was inoculated into the culture medium at 10% (v/v) and cultured in 250 mL Erlenmeyer flasks at 24 °C in a temperature-controlled room under continuous light (70 mmol photons per m^{-2} s^{-1}). The flask was stirred manually twice a day to prevent algal settlement.

Preparation of *Euglena gracilis* and TPE particle mixture

3 drops of *Euglena gracilis* culture media were added to the water–THF solutions (known water fractions) including TPE particles (either prepared traditionally or VFD-driven). At different time points, one drop of solution was poured into the cavity of a dual-cavity microscope slide and covered by a coverslip. The edges of the coverslip were covered with nail polish to minimize evaporation.

FL microscopy

An Olympus FL AX70 upright microscope with a Zeiss Axiocam 510 monochrome camera and Zen Blue Image Capture software was used for FL study. Light microscopic and FL images (excited at 365 and 470 nm) of *Euglena gracilis* and TPE particle mixture were captured. During excitation, appropriate matched emission wavelength filters were selected.

Image post-processing

ImageJ open source software was used for post-processing (pseudo-colouring) of images captured by the FL microscope. For post-processing, the image type was changed from RGB to binary (8-bit). Captured images under 365 and 470 nm excitations were coloured blue and green respectively, using look-up tables. No further adjustments for brightness or contrast were performed, and a multicolour composite image was created by merging associated images and converted to RGB format.

Scanning electron microscopy imaging

For SEM imaging (Inspect F50, FEI Company, USA) drops of samples including TPE particle solutions and *Euglena gracilis*

This journal is © The Royal Society of Chemistry and the Chinese Chemical Society 2020

Mater. Chem. Front., 2020, **4**, 537–545 | **543**

culture media were placed in turn on an aluminium stub. After complete drying in air, samples were sputter-coated with platinum at 2 nm thickness.

Fluorescence quantum yield measurement

The FL emission intensities were taken for samples prepared in water/THF ratio = 80% at different rotation speeds (0, 1000, 2000 and 3000 rpm), for water/THF ratio = 90% at 0 and 4000 rpm and for water/THF ratio= 60% at 4000 rpm, as explained before. The excitation wavelength was set at 350 nm. The area under emission peaks (integrated emission intensity) at different water/THF ratios and rotational speeds were calculated by using the spectrophotometer software (Cary Eclipse, Agilent Technologies). The absorbance of the samples at 350 nm was measured using UV-vis spectrophotometer (Cary 60, Agilent Technologies). Quinine sulphate (QS) was used as a reference with known quantum yield and refractive index values of 0.546 and 1.346, respectively. During measurement, in order to minimize the effect of the re-absorption, absorbance in the 10 mm cuvette was adjusted below 0.1 with an average of 0.085 ± 0.01. The absorbance for QS was measured as 0.0695. The refractive index for water and THF is 1.333 and 1.404 respectively. Therefore, the refractive index for the sample was averaged and estimated as 1.368. However, for the calculation of quantum yield, the ratio of refractive index for sample and reference was approximated as 1 (1.368/1.346 = 1.016).

Quantum yield for samples was calculated using the following equation:

$$\phi_s = \phi_r \times \frac{A_r}{A_s} \times \frac{IEI_s}{IEI_r} \times \frac{n_s^2}{n_r^2}$$

where ϕ, A, IEI and n represent quantum yield, absorbance, integrated emission intensity, and refractive index, respectively. s and r were used to identify sample and reference material (Quinine sulphate, QS) and the integrated emission intensity for QS was measured as 13 821 at 350 nm.

Measurement of stability of VFD-mediated TPE nanoparticles

The stability of the FL property for VFD-driven TPE nanoparticles was identified using a spectrophotometer. The FL intensity of nanoparticles at an excitation wavelength of 350 nm was recorded for as-prepared nanoparticles and compared to those were prepared after 5, 24, 300 and 480 hours. Moreover, images were captured using a camera under UV light (excitation wavelength = 365 nm).

Evaluation of crystallinity for VFD-mediated TPE nanoparticles

A polarizing microscope (Olympus, BH-2 series) with a blue light filter (KB-4) was used and microscopic images were captured using a colour camera (Olympus, DP20).

Conclusions

Overall, the preparation of TPE nanoparticles under thin film formation could support tuning their size and the associated intensity of FL. By increasing both water fraction and rotation speed during the preparation of TPE nanoparticles, the size of the particles can be controlled and significantly reduced, with the smaller particles increasing the brightness. The direct diffusion of nanoparticles within the cell or in a single-celled organism, as an advantage of size reduction, opens new opportunities for biological and material studies.

Conflicts of interest

There are no conflicts to declare.

Acknowledgements

Notes and references

1 R. Jakubiak, C. J. Collison, W. C. Wan, L. J. Rothberg and B. R. Hsieh, *J. Phys. Chem. A*, 1999, **103**(14), 2394–2398.

2 J. Mei, Y. Hong, J. W. Lam, A. Qin, Y. Tang and B. Z. Tang, *Adv. Mater.*, 2014, **26**(31), 5429–5479.

3 A. Qin, C. K. W. Jim, Y. Tang, J. W. Y. Lam, J. Liu, F. Mahtab, P. Gao and B. Z. Tang, *J. Phys. Chem. B*, 2008, **112**(31), 9281–9288.

4 Y. Liu, Y. Tang, N. N. Barashkov, I. S. Irgibaeva, J. W. Lam, R. Hu, D. Birimzhanova, Y. Yu and B. Z. Tang, *J. Am. Chem. Soc.*, 2010, **132**(40), 13951–13953.

5 Z. Wang, J. Nie, W. Qin, Q. Hu and B. Z. Tang, *Nat. Commun.*, 2016, **7**, 12033.

6 W. Z. Yuan, P. Lu, S. Chen, J. W. Lam, Z. Wang, Y. Liu, H. S. Kwok, Y. Ma and B. Z. Tang, *Adv. Mater.*, 2010, **22**(19), 2159–2163.

7 F. Guo, W.-P. Gai, Y. Hong, B. Z. Tang, J. Qin and Y. Tang, *Chem. Commun.*, 2015, **51**(97), 17257–17260.

8 J. Tavakoli, H.-p Zhang, B. Z. Tang and Y. Tang, *Mater. Chem. Front.*, 2019, **3**(4), 664–667.

9 J. Tavakoli, J. Gascooke, N. Xie, B. Z. Tang and Y. Tang, *ACS Appl. Polym. Mater.*, 2019, **1**(6), 1390–1398.

10 J. Tavakoli, E. Laisak, M. Gao and Y. Tang, *Mater. Sci. Eng., C*, 2019, **104**, 109951.

11 Y. Zhou, J. Hua, G. Barritt, Y. Liu, B. Z. Tang and Y. Tang, *ChemBioChem*, 2019, **20**(10), 1256–1259.

12 D. Wang, J. Qian, W. Qin, A. Qin, B. Z. Tang and S. He, *Sci. Rep.*, 2014, **4**, 4279.

13 M. Zhao, Z. Qian, M. Zhong, Z. Chen, H. Ao and H. Feng, *ACS Appl. Mater. Interfaces*, 2017, **9**(38), 32887–32895.

14 H. Zhang, X. Zheng, R. T. K. Kwok, J. Wang, N. L. C. Leung, L. Shi, J. Z. Sun, Z. Tang, J. W. Y. Lam, A. Qin and B. Z. Tang, *Nat. Commun.*, 2018, **9**(1), 4961.

15 S. A. Fateminia, Z. Wang, C. C. Goh, P. N. Manghnani, W. Wu, D. Mao, L. G. Ng, Z. Zhao, B. Z. Tang and B. Liu, *Adv. Mater.*, 2017, **29**(1), 1604100.

16 J. Britton, K. A. Stubbs, G. A. Weiss and C. L. Raston, *Chem. – Eur. J.*, 2017, **23**(54), 13270–13278.

17 K. Vimalanathan, J. R. Gascooke, I. Suarez-Martinez, N. A. Marks, H. Kumari, C. J. Garvey, J. L. Atwood, W. D. Lawrance and C. L. Raston, *Sci. Rep.*, 2016, **6**, 22865.

18 X. Luo, A. H. M. Al-Antaki, K. Vimalanathan, J. Moffatt, K. Zheng, Y. Zou, J. Zou, X. Duan, R. N. Lamb and S. Wang, *React. Chem. Eng.*, 2018, **3**(2), 164–170.

19 X. Luo, P. Smith, C. Raston and W. Zhang, *ACS Sustainable Chem. Eng.*, 2016, **4**(7), 3905–3911.

20 X. Luo, A. H. M. Al-Antaki, S. Pye, R. Meech, W. Zhang and C. L. Raston, *ChemPhotoChem*, 2018, **2**(4), 343–348.

21 X. Chen, J. F. Dobson and C. L. Raston, *Chem. Commun.*, 2012, **48**(31), 3703–3705.

22 T. Z. Yuan, C. F. Ormonde, S. T. Kudlacek, S. Kunche, J. N. Smith, W. A. Brown, K. M. Pugliese, T. J. Olsen, M. Iftikhar and C. L. Raston, *ChemBioChem*, 2015, **16**(3), 393–396.

23 K. Vimalanathan and C. L. Raston, *Adv. Mater. Technol.*, 2017, **2**(6), 1600298.

24 Y. Dong, J. W. Y. Lam, A. Qin, J. Liu, Z. Li, B. Z. Tang, J. Sun and H. S. Kwok, *Appl. Phys. Lett.*, 2007, **91**(1), 011111.

25 Y. Jiang, T. He, Y. Chen, Y. Ruan, Y. Zhou, B. Z. Tang, J. Qin and Y. Tang, *Environ. Sci.: Nano*, 2017, **4**(11), 2186–2192.

26 J. S. Brown, *Biochim. Biophys. Acta, Bioenerg.*, 1980, **591**(1), 9–21.